High Sensitivity of Zn^{2+} Insulin to Metal-Catalyzed Oxidation: Detection of 2-Oxo-Histidine by Tandem Mass Spectrometry

Susan W. Hovorka,[1] Homigol Biesiada,[2] Todd D. Williams,[2] Andreas Hühmer,[3] and Christian Schöneich[1,4]

Received December 14, 2001; accepted January 4, 2002

Purpose. To establish the sensitivity of Zn^{2+} insulin (Zn^{2+}-INS) to metal-catalyzed oxidation (MCO) and to use tandem mass spectrometry/mass spectroscopy (MS/MS) for the identification and quantification of 2-oxo-histidine at $^{5}His_{B}$ and $^{10}His_{B}$ upon the MCO of INS.
Methods. Zn^{2+}-INS was exposed to Cu^{2+}/ascorbate-induced MCO. Products were analyzed by reverse-phase high-performance liquid chromatography, electrospray ionization mass spectrometry (ESI-MS) and MS/MS, sodium dodecylsulfate polyacrylamide gel electrophotesis (SDS-PAGE), and CD spectroscopy.
Results. A maximal loss of 40% INS was achieved when 20 μM INS/8.8μM Zn^{2+} were exposed to 8 μM Cu^{2+} and 50 μM ascorbate. MCO was completely inhibited by ethylenediaminetetraacetic acid or native catalase but not with a 1000-fold molar excess of Zn^{2+} over Cu^{2+}. MCO did not alter the aggregation state of INS. High-performance liquid chromatography-fractionated products contained portions of oxidized and native INS monomers. Oxidation selectively targeted the B chain of INS, where MS/MS sequencing revealed 2-oxo-His formation at both His residues at a relative ratio of $^{10}His_{B\text{-}ox}/^{5}His_{B\text{-}ox} = 2.8 \pm 1.3$ (SD).
Conclusions. At a Zn^{2+}/INS molar ratio comparable to that in regular INS preparations, Zn^{2+}-INS was susceptible to MCO. Both His residues of INS were converted partially to 2-oxo-His, with $^{10}His_{B}$ possessing ca. three times greater susceptibility to MCO than $^{5}His_{B}$.

KEY WORDS: insulin; zinc-insulin; metal-catalyzed oxidation; 2-oxo-histidine.

INTRODUCTION

Transition metals are present in most buffers and may affect the processing and/or storage of biologic pharmaceuticals. Therefore, metal-catalyzed oxidation (MCO) (1,2) poses a serious threat to the stability of recombinant proteins. The metal-binding amino acids are particularly sensitive to MCO. For example, His is converted to 2-oxo-histidine (2-oxo-His) in the presence of Cu^{2+} and ascorbate (3,4). Scheme I (5,6) presents a mechanism for the formation of 2-oxo-His by reaction of His with the hydroxyl radical, HO•. Here, HO• is generated at the metal-binding site via one-electron reduction

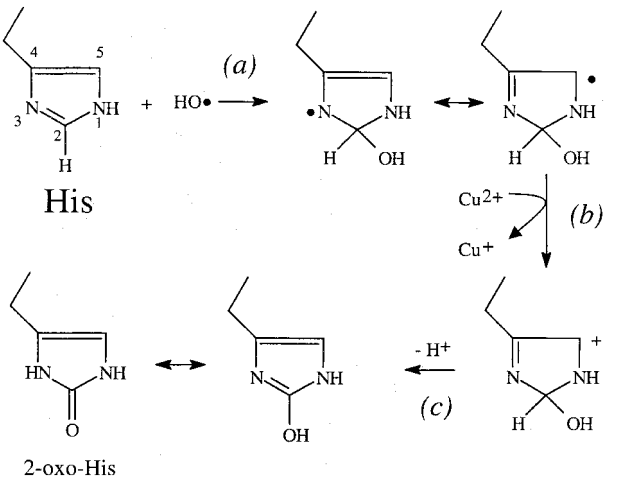

Scheme I.

of a redox active transition metal and subsequent one-electron reduction of freely diffusable H_2O_2. H_2O_2 results from a series of redox reactions between liganded reduced transition metals, e.g., L_x-Cu^{1+}(5) and L_x-Fe^{2+} (7), and molecular oxygen. Identification of 2-oxo-His by traditional methods, i.e., amino acid analysis, has proven to be difficult, but has been achieved by high-performance liquid chromatography (HPLC) with electrochemical detection (4), modified amino acid analysis (8), and by MS/MS (9), which is also the method of detection used in the present work. The Cu^{2+}/ascorbate-induced formation of 2-oxo-His has been reported for the following protein pharmaceuticals: human growth hormone (hGH) (5), bovine growth hormone (bGH) (9), human relaxin (10,11), and brain-derived neurotrophic factor (12). Furthermore, 2-oxo-His has been detected during metal-catalyzed photodegradation of human growth hormone (13). However, all of these studies were performed in aqueous model systems, which are limited in relevance to typical protein formulations. To study MCO under formulation-like conditions, the present report details the MCO of insulin (INS), one of the most well-studied and applicable of the protein pharmaceuticals (14–16), at INS/Zn^{2+} molar ratios similar to those found in regular INS preparations (15).

The B chain of the INS monomer contains two His residues, $^{5}His_{B}$ and $^{10}His_{B}$. In the presence of Zn^{2+}, three INS dimers aggregate into a torus-shaped hexamer with two Zn^{2+} binding sites. Each binding site is comprised of three $^{10}His_{B}$ imidazole ligands (17), with the corresponding $^{5}His_{B}$ residues in close proximity (Fig. 1). Two previous studies (18,19) have exposed INS to Cu^{2+} and/or ascorbate, but both were ambiguous as to the Zn^{2+} content of the protein and none of them identified the oxidation products of His. Although Cheng and Kawakishi (19) detected a greater loss of $^{10}His_{B}$ than $^{5}His_{B}$ in oxidized products, the differential susceptibility of $^{5}His_{B}$ and $^{10}His_{B}$ to MCO has yet to be quantitated.

In this report, the MCO of INS was performed at INS/Zn^{2+} molar ratios of ca. 2/1, which is similar to the INS/Zn^{2+} molar ratio of INS formulations. Regular INS preparations contain 0.60 mM (3.5 mg/mL) INS and 0.27 mM (20 μg/mL) Zn^{2+} (15), resulting in a molar ratio of ca. 2 INS/1 Zn^{2+}. Typical INS formulations also contain helix-stabilizing agents, such as phenol (15); however, such components were not

[1] Department of Pharmaceutical Chemistry, University of Kansas, Lawrence, Kansas 66047.
[2] Mass Spectrometry Laboratory, Univeristy of Kansas, Lawrence, Kansas 66045.
[3] Proteomic Technologies, ThermoFinnigan Corporation, San Jose, California 95134.
[4] To whom correspondence should be addressed. (e-mail schoneic@ukans.edu)

0724-8741/02/0400-0530/0 © 2002 Plenum Publishing Corporation

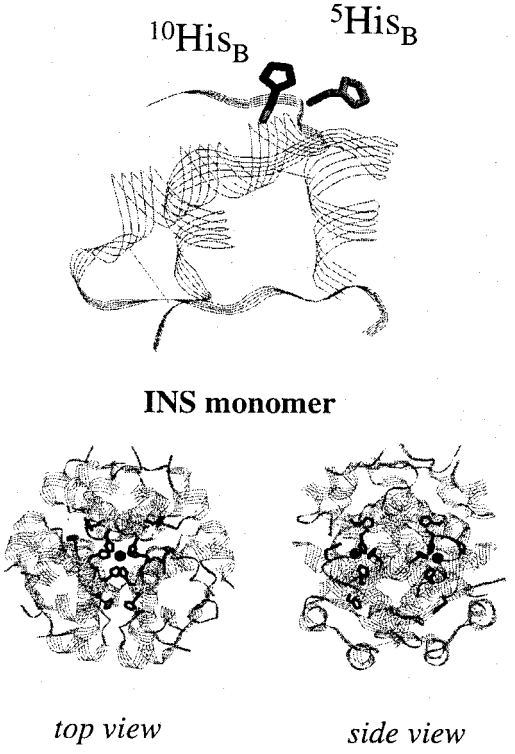

Fig. 1. Structure of the INS monomer (adapted from PDB file 4INS) and hexamer (PDB file 1WAV), where $^{5}His_B$ is in gray and $^{10}His_B$ is in black.

added in this study. An electron paramagnetic resonance (EPR) study of Cu^{2+}-INS revealed that Cu^{2+} binds to the same binding sites as Zn^{2+} in the hexamer (20). Zn^{2+}, a redox inert metal, should compete with Cu^{2+} for the metal-binding sites in the INS hexamer and, in large excess, may competitively inhibit MCO. However, the following study will demonstrate that even in the presence of a large molar excess of Zn^{2+} over Cu^{2+}, INS is sensitive to MCO. Tandem mass spectroscopy (MS/MS) experiments were used to identify 2-oxo-His formation at both His residues of INS, and to establish the differential sensitivity of $^{5}His_B$ and $^{10}His_B$ towards oxidation. In this way, the potential for MCO as a degradation pathway for INS under formulation conditions will be ascertained.

EXPERIMENTAL

Materials

Recombinant human INS, with a content of Zn^{2+} that is ~0.5% of the weight of amorphous dry INS, was purchased from ICN Biomedicals, Inc. (Costa Mesa, CA), and the B chain of INS, in which both Cys have been oxidized to cysteic acid, was purchased from Sigma-Aldrich (St. Louis, MO). Unless otherwise stated, all reagents were of the highest grade commercially available. To ensure adequate solubility, stock solutions of INS, the B chain of INS, and $ZnCl_2$ were prepared in 0.1 N HCl. Concentrations of INS and the B chain were determined spectrophotometrically [$\varepsilon_{275nm} = 5988\ M^{-1}$ and $\varepsilon_{276nm} = 3100\ M^{-1}$, respectively (21)]. Stock solutions of INS, ascorbate, $CuCl_2$, $ZnCl_2$, and catalase were prepared immediately before experimentation.

Reaction Conditions

Reactions were performed at room temperature and consisted of 500-μL solutions containing 20 μM INS, 8.8 μM Zn^{2+}, 0.8 or 8 μM Cu^{2+}, and 50 μM ascorbate in 20 mM sodium phosphate buffer (pH 7.4). The order of reactant addition was as follows: Zn^{2+}-INS, water, buffer, Cu^{2+}, and finally, after a 10-min lag phase to promote the binding of metal to INS, ascorbate. In some experiments, exogenously added $ZnCl_2$, ethylenediaminetetraacetic acid (EDTA), or catalase was added prior to the lag phase. To ensure an adequate supply of oxygen throughout the course of reaction, reagents were placed in clear 1.5-mL dram vials capped with teflon-lined lids (Kimble Glass, Inc.; Vineland, NJ). Experimental controls were performed in the absence of ascorbate.

For characterization of the oxidation products, INS was reduced and alkylated. The disulfide bonds of INS were reduced by 3 mM DTT at 37°C for 30 min in the presence of 6 M guanidine hydrochloride, 200 mM trishydroxymethylaminomethane (pH 8.3), and 2 mM EDTA. Free thiols were alkylated with 5 mM iodoacetic acid in the dark for 30 m at 37°C. Finally, excess iodoacetic acid was reacted with 0.14 M (i.e., 1% v/v) β-mercaptoethanol.

HPLC Analysis

Reaction mixtures were separated by reverse-phase (RP)-HPLC on a Vydac C4 column (250 × 4.6 mm id; Vydac; Hesperia, CA) using a linear acetonitrile/trifluoroacetic acid gradient with UV detection at 214 nm and a flow rate of 1 mL/min. The mobile phase ratio started with 100% mobile phase A [A = 25% (v/v) acetonitrile/0.1% (v/v) trifluoroacetic acid] at 0 min and was increased linearly to 100% B [B = 50% (v/v) acetonitrile/0.1% (v/v) trifluoroacetic acid] within 12.5 min. The HPLC system consisted of two Shimadzu LC-10AS pumps and a Shimadzu SPD-10AV UV/vis detector (Shimadzu; Columbia, MD). Data are reported as the ratio of the average peak area of the analyte at time x to the average peak area of INS at time 0 [equation 1].

$$\text{Fraction of INS} = \langle\text{peak area}\rangle_{t=x} / \langle\text{INS area}\rangle_{t=0} \quad (1)$$

ESI-Q-TOF MS and MS/MS

Before mass spectral analysis, lyophilized samples were desalted by dissolution in 50% acetic acid, followed by dilution to 1% acetic acid and injection onto a C18 guard column (1 × 20 mm (Upchurch Scientific model C.128, Oak Harbor, WA) that was dry-packed with Zorbax C18 resin (SBC18, 5uM, 300A, Rockland Technologies, Newport, DE) for trapping. Desalted samples were either directly analyzed by elution off the C18 column with 90% methanol/1% formic acid into the ESI source for MS, or were collected and pooled for minute-long infusions for MS/MS. ESI-MS spectra were acquired on a Q-TOF-2 (Micromass Ltd., Manchester UK) hybrid mass spectrometer operated in the MS mode with data acquisition by the time of flight (TOF) analyzer. The instrument was operated at isotopic resolution. The cone voltage was 30 eV and the cell was operated at 10 eV (maximum transmission).

Collision induced dissociation (CID) spectra were acquired by setting the MS1 quadrupole to transmit a precursor mass window of ±1.5 a.m.u. centered on the most abundant isotopomer of the MH_4^{4+} ion. The collision energy was varied from 20 to 35 eV over 5 min of acquisition time.

Spectra were manipulated for data analysis in the following ways. Multiple-charged spectra were converted to singly charged spectra with the MaxEnt 3 software (Micromass Ltd.; Manchester, UK). This simplified the interpretation of MS/MS data since CID spectra from the multiply charged precursor ion (+4) result in a suite of multiply charged product ions with z = +2 and +3. The ions in each CID spectra were normalized to the signal at m/z 226.13, an abundant ion for all spectra representing the internal fragment ^{28}ProLys. The normalized a, b, and y ions, where a, b, and y are defined by Roepstorff's nomenclature (22), were compared between CID spectra to ascertain the extent of oxidation at each position (see Results for further detail).

ESI-Ion Trap-MS/MS

Further MS analyses of control and oxidized INS were performed by Ion Trap MS on either a Deca or Deca XP ion trap mass spectrometer (ThermoFinnigan; San Jose, CA). INS and oxidized INS samples were reduced, alkylated (see above), and desalted. Samples were analyzed in two different nanospray modes using a Nanospray source (Thermo Finnigan). For the static nanospray experiments, 2 μL of the sample was loaded into a metal-coated glass PicoTip with a 2-μm tip ID (New Objective, Woburn, MA) and sprayed at 1.8 kV without the aid of an additional pump or pressure source. For dynamic nanospray experiments, 2-μL aliquots of the samples were injected onto a 180 μm ID × 10 mm Hypurity column (Thermo Hypersil) and separated from salt with a 30 min gradient from 5% mobile phase B to 95% B (mobile phase A = 0.1% aqueous formic acid and B = AcN with 0.1% formic acid) using a Surveyor gradient HPLC system (Thermo Finnigan, San Jose, CA). The column eluent was introduced into the mass spectrometer using a fused-silica PicoTip with a 30 μm ID at a flow rate of 1μL/min. Data were recorded in full MS and data-dependent MS/MS and single ion monitoring in full MS and MS/MS mode were conducted on the +3, +4, and +5 m/z species using collision energies between 35% and 60%.

SDS–PAGE

Gel electrophoresis was performed using pre-cast 4–20% tris-glycine minigels (1.5 mm × 10 wells; Novex; San Diego, CA) at 12°C. One-milliliter reaction mixtures were lyophilized and, subsequently, dissolved in tris-glycine/SDS sample buffer (Novex) containing bromophenol blue, and incubated at 95°C for 5 min. Novex Mark 12 wide-range standard was used for the approximation of molecular weight. After electrophoresis, gels were stained with Coomassie Blue R-250 for 2 h and destained in 40% (v/v) methanol and 7.5% (v/v) acetic acid overnight.

CD Spectroscopy

Far UV CD spectra were acquired on a Jasco J-720 spectrometer (Jasco; Easton, MD) at 25°C and were the average of three replicate scans. Protein samples (20 μM) were placed in a 0.1-cm pathlength quartz cuvette and monitored every 0.1 nm at a speed of 20 nm/min from 260 to 180 nm. CD spectra were deconvoluted into helix, β-sheet, turn and/or random structural components by three different algorithms (Selcon, CD Estima and Contin; 23).

RESULTS

Loss of INS

Upon exposure of 20 μM INS and 8.8 μM Zn^{2+} to either 0.8 or 8 μM Cu^{2+} and 50 μM ascorbate, INS degraded to the extent of 10 or 40% within 90 min, respectively (Fig. 2B). Concentrations of >50 μM ascorbate failed to increase the overall loss of INS (data not shown). The oxidation products were separated by HPLC into five fractions (Fig. 2A) that accounted for 100% of protein loss. Initial experiments with the B chain of INS showed a maximum loss of ca. 25% under the same conditions (data not shown).

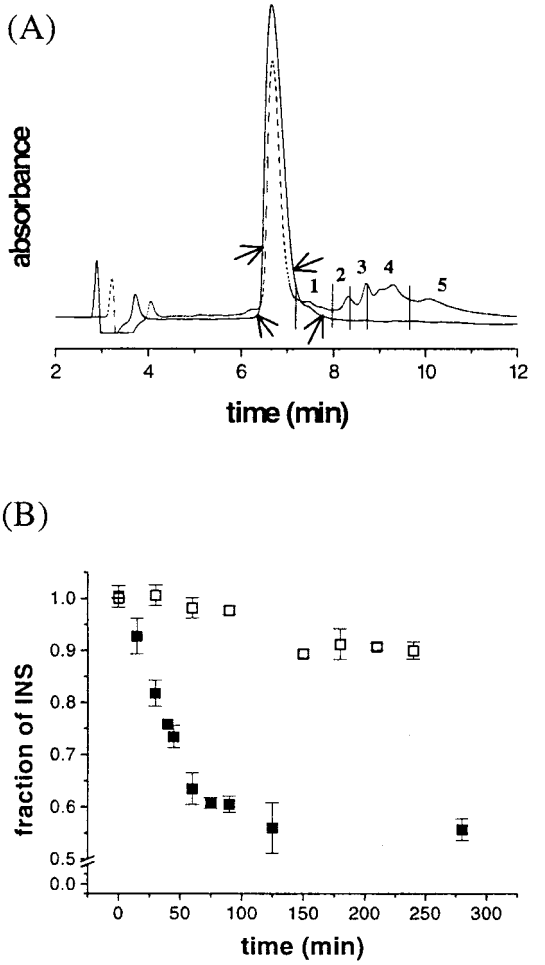

Fig. 2. Chromatogram and kinetic time course for the MCO of Zn^{2+}-INS. (A) Chromatographic overlay of oxidized (dashed line) and control (solid line) Zn^{2+}-INS. The chromatogram of the control sample is further indicated by the inserted arrows. (B) Kinetic profile for the reaction of 20 μM INS/8.8 μM Zn^{2+} with 8 μM (closed squares) or 0.8 μM Cu^{2+} (open squares) and 50 μM ascorbate in 20 mM sodium phosphate (pH 7.4) at room temperature (see Eq. 1 for quantitation). For oxidation conditions, see Experimental section.

The MCO of INS was completely inhibited in the absence of ascorbate by the addition of 50 μM EDTA or by the addition of 2000 units of native catalase, whereas heat-denatured catalase had no effect on the reaction. In an attempt to competitively inhibit Cu^{2+}-binding, exogenous $ZnCl_2$ was added before the addition of 0.8 μM Cu^{2+}. At a Zn^{2+} concentration of 800 μM, oxidation products were just beginning to appear after two hours of reaction, demonstrating slower oxidation kinetics; however, these data show that even a molar ratio of 1 Cu^{2+}/1000 Zn^{2+} was unable to prevent oxidation. The addition of Zn^{2+} in the mM-range was difficult due to the precipitation of $Zn(OH)_2$ at pH 7.4.

Product Characterization

Separation of A and B Chains

Reduction and alkylation of INS yields alkylated A and B chains, which can be separated by HPLC. Comparison of the A and B chains shows that oxidation exclusively targets the B chain to an extent of 40% (Fig. 3), i.e., similar to the loss observed for whole INS (Fig. 2B). Both His residues of INS, $^{5}His_B$, and $^{10}His_B$ are located on the B chain.

ESI-Q-TOF MS of Whole Protein

Using the higher mass resolution capability of the Q-TOF configuration, the molecular weights of the species contained in product regions 1–5 (defined in Fig. 2A) were determined by ESI-Q-TOF MS. Products 1–5 were found to contain mixtures of the following average masses (M_r): INS (M_r = 5807.7), INS + 16 a.m.u. (M_r = 5823.7), and INS + 32 a.m.u. (M_r = 5839.7). Table I reports the relative ratios of the INS species contained in each product region, which were normalized to the INS signal in Product 4. Product 4 contains the greatest yields of mono-oxidized (INS + 16 a.m.u.) and di-oxidized (INS + 32 a.m.u.) species. Assuming that the addition of 16 a.m.u. represents the addition of one oxygen atom, all products of MCO are the result of oxygen addition. All product fractions contain a portion of native INS monomer. Because Zn^{2+}-INS is in the hexameric state, it is apparent that not all of the six INS monomers of the hexamer are covalently modified by MCO. Furthermore, INS does not contain Met residues. Thus, the formation of mono-oxidized INS cannot be due to the formation of methionine sulfoxide.

ESI-Q-TOF MS/MS and ESI-Ion Trap-MS/MS

Considering that only the B chain of INS is affected by MCO and that both His residues of INS are located on this chain, the oxidized B chain was sequenced using ESI-Q-TOF MS/MS. Reaction mixtures were reduced by a molar excess of ca. 1500 DTT over total protein, then immediately desalted, collected, and pooled for infusion into the Q-TOF-2 MS. Note that, due to the excess of DTT to total protein, the samples were not alkylated prior to MS analysis. CID experiments were performed on the following quadruply charged ions, originating from the addition of four protons to the respective peptides: MH_4^{4+} = 857.9, corresponding to the monoisotopic mass of the native B chain, MH_4^{4+} = 861.9, corresponding to B chain + 16 a.m.u. (mono-oxidized B chain), and MH_4^{4+} = 865.9, corresponding to the B chain + 32 a.m.u. (di-oxidized B chain). Scheme II, upper panel, presents those ions observed

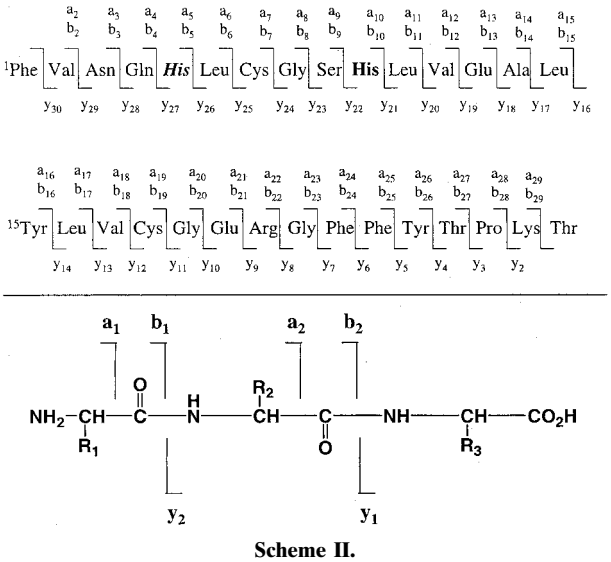

Scheme II.

in the CID spectra for the B chain of INS. The lower panel indicates the exact cleavage sites for a model peptide structure, producing a, b, and y ions (usually present as y") (24). In Scheme II, the two His are highlighted and distinguished by font to indicate which fragment ions would differentiate oxidation at $^{5}His_B$ from that of $^{10}His_B$.

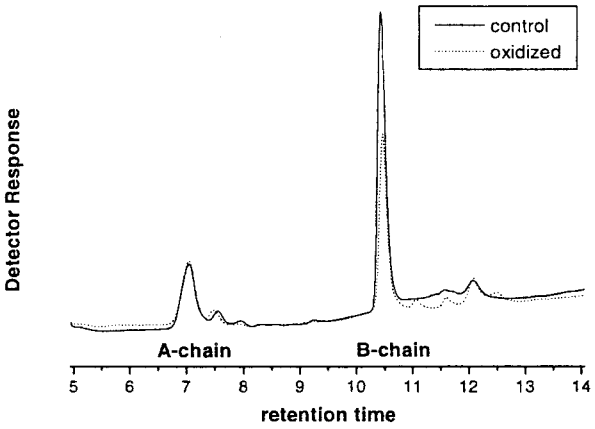

Fig. 3. A and B peptide chains of an oxidized (dashed line) and control (solid line) reaction mixture of 20 μM INS with 8.8 μM Zn^{2+} exposed to 8 μM Cu^{2+} and 50 μM ascorbate in 20 mM phosphate (pH 7.4). For details on the separation conditions, see Experimental section.

Table I. Relative Ratios of INS Species in Products 1–5[a]

	Relative product ratios		
Product	INS	+16	+32
1	0.5	0.3	0.2
2	0.2	0.6	0.2
3	0.2	0.2	0.1
4	1.0	0.7	1.0
5	0.2	0.2	0.2

[a] The ratios are relative to the most abundant species, which was INS in product 4.

MS/MS of the Mono-Oxidized B Chain (MH_4^{4+} = 861.9) Full a, b, and y series corresponding to oxidation at either $^{5}His_B$ or $^{10}His_B$ were detected in the CID spectra for MH_4^{4+} = 861.9. Although the spectra indicate that the His residues were the most abundant sites for oxidation, other amino acids in the sequence are also theoretically labile towards oxidation, i.e., Cys, Tyr, and Phe. To determine whether oxidation occurred at these other sites, the relative abundances of a, b, and y fragments were compared to the relative abundances of the respective fragments in the MS/MS spectra for the native B chain (MH_4^{4+} = 857.9). This ratio is termed the "relative ion ratio" in Fig. 4. Ratios near one indicate the absence of oxidation in a particular fragment, while ratios well below one indicate the occurrence of oxidation. For example, b_2 (Fig. 4B) is not oxidized in either CID spectrum; thus, dividing the normalized intensity of b_2 from the CID spectrum of the mono-oxidized B-chain by b_2 from CID spectra of the native B chain yields a value close to one. Conversely, the signal for b_5 (Fig. 4B) in the CID for the mono-oxidized B chain is about one-fourth of that for b_5 in the native B-chain. Thus, this relative ion ratio is much less than one and signifies that a residue in this fragment has been covalently modified.

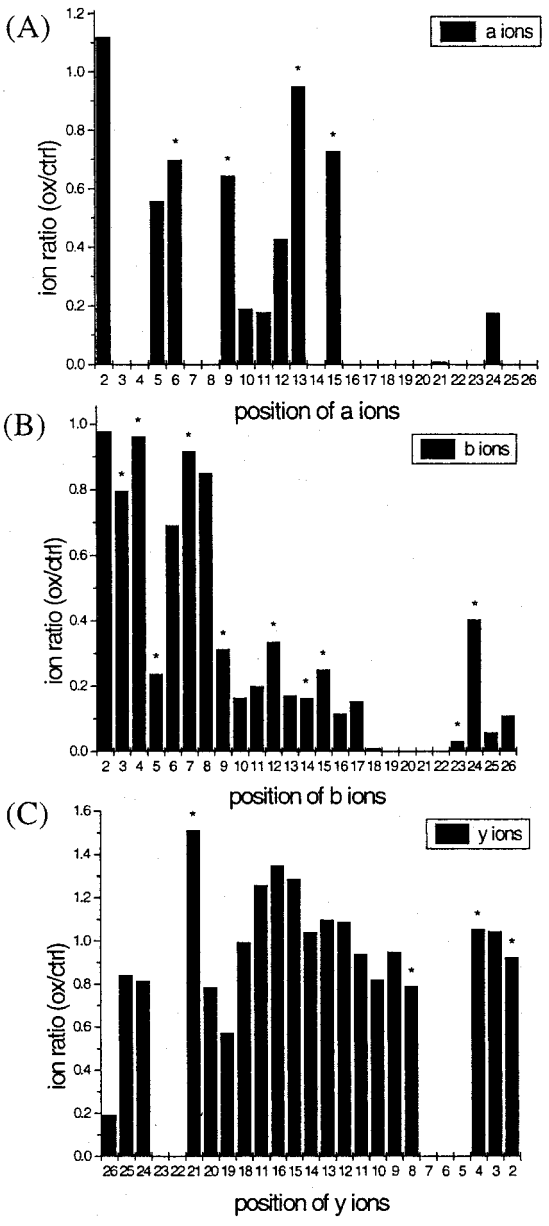

Fig. 4. (A), (B), and (C) represent the relative ion ratios of a, b, and y ions, respectively, in the mono-oxidized MS/MS (MH_4^{4+} = 861.9) relative to the respective ion signals in the native MS/MS (MH_4^{4+} = 857.9). MS/MS ions that are isobaric with internal acyl fragments are marked with '*' and may not necessarily represent signals that are specific to one ion.

Figure 4 presents the relative ion ratios for the a, b, and y ions (Fig. 4A, B, and C, respectively). Ratios marked with an asterisk indicate that the m/z value for the ion coincides with that of an internal fragment (an internal fragment can form when a primary charged fragment suffers a second cleavage process generating a charged fragment which neither contains the N- or C-terminus of the original peptide); thus, these ratios may not be entirely specific for that particular ion. Examination of Fig. 4, A and B reveal that mild oxidation occurs at and after residue 5 but before residue 10, and that a greater extent of oxidation occurs at and after residue 10. This suggests that $^{10}His_B$ is the major site for oxidation and that $^{5}His_B$ is oxidized to a lesser extent. Figure 4C shows relative ion ratios near unity for most of the y ions, except for y''_{26}, which represents the fragment with $^{5}His_B$ at the N-terminus, suggesting predominant oxidation at $^{5}His_B$. However, the y fragment with $^{10}His_B$, at the N-terminus, y''_{21}, is isobaric with an internal fragment and is not necessarily specific for y''_{21}. Figures 4A and 4B indicate that the majority of the oxidation occurs at $^{10}His_B$ in the mono-oxidized B chain, while Figure 4C is ambiguous. Nonetheless, it is apparent from Fig. 4 that oxidation in the mono-oxidized B-chain is specific to either $^{5}His_B$ or $^{10}His_B$ and not to any other amino acid residue. This specificity was confirmed by ESI-Ion Trap-MS/MS of the reduced and alkylated mono-oxidized B chain (data not shown).

Oxidation at either $^{5}His_B$ or $^{10}His_B$ produces a different series of ions between a_5-a_9 and b_5-b_9. Comparison of the intensities for each set of ions can be used as a quantitative measure of oxidation at either site. The bolded ions located in the inset of Fig. 5 were used for such quantitation (the unbolded ions were not used since they are isobaric with internal fragments). The stick diagram in Figure 5 gives an example of the ion intensities for the two a_5 + 16 a.m.u. ions and the two b_6 + 16 a.m.u. ions. Note that the MS/MS experiment was performed on the monooxidized B-chain. The fragment with m/z 598.3 represents the a_5 ion corresponding to the non-oxidized sequence Phe^1-Val-Asn-Gln-His^5; hence the intensity of this unmodified fragment derived from the monooxidized B-chain quantitatively represents oxidation at His^{10} (because His is the exclusive target of oxidation). On the other hand, the fragment ion with m/z 614.3 represents the monooxidized sequence Phe^1-Val-Asn-Gln-His^5(O); hence, the intensity of this ion quantitatively represents oxidation at His^5. A similar consideration applies to the b_6 ions. Table II lists the intensity ratios for each set of ions and yields an average ratio of oxidation at $^{10}His_B/^{5}His_B$ of 2.8 ± 1.3 (SD).

MS/MS of the Di-Oxidized B Chain (MH_4^{4+} = 865.9) ESI-Q-TOF-MS/MS investigation of the di-oxidized B chain (MH_4^{4+} = 865.9) revealed the following abundant fragments that suggest simultaneous oxidation at $^{5}His_B$ and $^{10}His_B$: a_{10} +

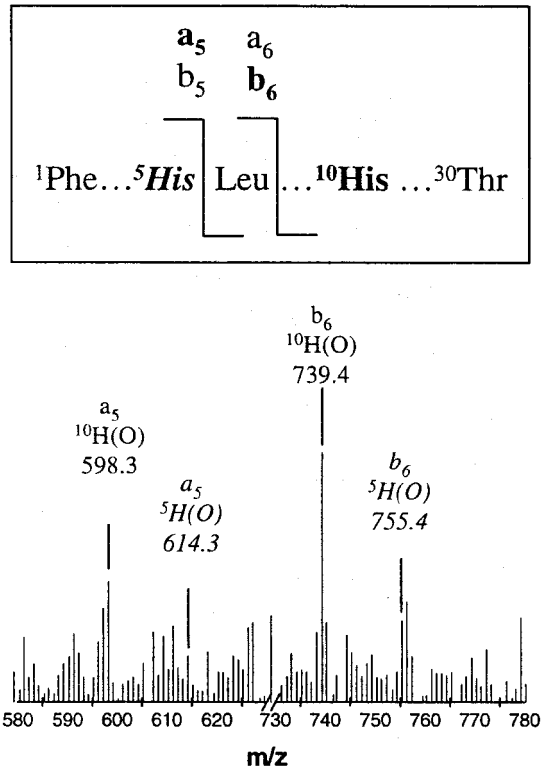

Fig. 5. MS/MS from 580 to 780 m/z for the mono-oxidized B-chain of INS (MH_4^{4+} = 861.9). Inset: Sequence between position 5 and 10 with the a and b ions that were used to quantitate oxidation at $^{5}His_B$ vs. $^{10}His_B$ in bold. Oxidation at $^{5}His_B$ is distinguished from $^{10}His_B$ by the use of italics.

32 a.m.u. (MH^+ = 1127.4), b_{10} + 32 a.m.u. (MH^+ = 1155.4), and y''_{26} + 32 a.m.u. (MH^+ = 2972.5).

SDS-PAGE

Oxidized Zn^{2+}-INS samples, in which the concentration of Cu^{2+} was 8 μM, and control reaction mixtures, were lyophilized and electrophoresed on 4–20% tris-gly gels. There was no difference in band migration between the oxidized and control samples (data not shown). Bands in each sample corresponded to molecular weights of monomeric INS and other aggregated forms, i.e., dimer and tetramer. The INS hexamer was not observed in either lane, but this is most likely due to a dilution effect. Importantly, however, MCO of Zn^{2+}-INS under these conditions does not seem to affect the oligomeric state.

CD Spectroscopy

Far-UV CD spectroscopy was used to determine whether MCO altered the secondary structure of Zn^{2+}-INS. There was no visible difference between the spectra of INS exposed to MCO and the control (data not shown). The lack of secondary structural perturbation was also evident when the spectra were deconvoluted. Structural contents of the control and oxidized spectra were not significantly different (data not shown).

DISCUSSION

Sensitivity of Zn^{2+}-INS to MCO

The MCO of Zn^{2+}-INS, at concentrations of 20 μM INS and 8.8 μM Zn^{2+}, with 50 μM ascorbate was performed at two separate molar ratios of Cu^{2+}/Zn^{2+}, ca. 1/1 and 1/10, and led to 40% and 10% loss of INS, respectively (Fig. 2B). Even when Cu^{2+}/Zn^{2+} was decreased to 1/1000 by the addition of exogenous $ZnCl_2$, Zn^{2+} was unable to completely inhibit MCO. This suggests that INS has a significantly stronger affinity to Cu^{2+} than Zn^{2+}. For comparison, in the case of hGH, MCO was entirely inhibited by a molar excess of 80 Zn^{2+}/1 Cu^{2+} (5). Thus, INS appears to be extremely sensitive to MCO even under conditions that could possibly be due to metal-contamination of a formulation. For example, the concentrations for INS and Zn^{2+} in most regular INS preparations are ca. 600 and 300 μM (15), respectively, and the concentration of residual Cu^{2+} contamination of 50 mM phosphate buffer is ca. 0.13 μM (25). If a regular INS preparation is contaminated with 0.13 μM Cu^{2+}, Zn^{2+} would be in 2300 molar excess over Cu^{2+}.

Table III compares the sensitivity of Zn^{2+}-INS to MCO with the sensitivities of other pharmaceutically relevant proteins. If the ascorbate/protein value in Table 3 is taken as an indicator of the susceptibility of the protein to MCO, where a low value indicates high susceptibility, Zn^{2+}-INS appears as one of the most susceptible of any of the proteins investigated. We note that the concentration of Zn^{2+}-INS in Table III is based on monomeric INS. In the presence of micromolar concentrations of Zn^{2+}, the aggregation state of INS is predominantly hexameric; thus the "true" concentration of Zn^{2+}-

Table II. Relative Intensities of Signals for Oxidation at $^{5}His_B$ vs. $^{10}His_b$ for Key at and b Ions.

Fragment	Peak area,[a] $^{10}His_B(O)$	Peak area,[a] $^{5}His_B(O)$	$^{10}His_B(O)/^{5}His_B(O)$
a_5	6.95	2.66	2.6
b_6	1.45	0.47	3.1
a_7	1.47	1.03	1.4
a_8	1.42	0.67	2.1
b_8	7.29	1.51	4.8
average ± SD			2.8 ± 1.3

[a] In % relative to the ion with m/z 226.13, the most abundant ion in all spectra, representing the internal fragment 28ProLys.

Table III. Survey of Various Cu^{2+}/Ascorbate-Induced MCO Studies

	Protein (μM)	Cu^{2+} (μM)	Ascorbate (μM)	Ascorbate/ protein	Percent protein remaining after MCO
hGH[a]	18	10	100	5.6	~5%
bGH[b]	9	5	50	5.6	nd
BDNF[c]	20	20	2000	100	65%
hRLX[d]	16.7	20	2000	120	~0%
Zn^{2+}-INS	20	8	50	2.5	60%

[a] Reference (5).
[b] Reference (9).
[c] Reference (10).
[d] Reference (12).

INS in Table III should be 3.3 μM and the ascorbate/protein value is 16.7. Despite this fact, Zn^{2+}-INS is still highly susceptible to MCO, especially when one considers that MCO is not completely inhibited through competition by Zn^{2+}.

The inhibition of MCO by 50 μM EDTA and 2000 U/mL catalase warrants discussion. Because EDTA will chelate both Cu^{2+} and Zn^{2+}, the mechanism of MCO-inhibition imparted by EDTA could be due to sequestering the redox-active metal (i.e., Cu^{2+}) and/or to driving the INS equilibria from the hexameric to the dimeric form. [At a concentration of 20 μM and in the absence of any divalent metal, INS should be predominantly in the dimeric form (26).] The utilization of 2000 U/mL of catalase to dismutate H_2O_2 may seem excessive, but, for comparison, a high concentration of catalase (1000 U/mL) was necessary to totally inhibit the MCO of hRLX (10). Furthermore, Inoue and Hiroba noted only a 15% decrease in MCO of INS upon the addition of 128 U/mL catalase (18).

The B chain of INS, in which both Cys were oxidized to cysteic acid, was sensitive to MCO. In aqueous solution, the B chain is known to form a right-handed helix (15), making it impossible for both His to be on the same face of the helix and simultaneously bind to one Cu^{2+} atom. At this point, the method by which the B chain binds to Cu^{2+} is unclear. Possibilities include the formation of a binding site comprised of imidazole ligands from more than one B chain, or the transient binding of His to Cu^{2+}. Further analysis of the conformational requirements for the MCO of the B chain, especially with regard to quantitation of oxidation at $^{5}His_B$ and $^{10}His_B$, are in progress.

Product Characterization

The oxidation products of Zn^{2+}-INS accounted for 100% of lost INS. Each product fraction (Figure 2A) contains native INS monomer, as determined by ESI-Q-TOF-MS (Table I), suggesting that not all of the INS monomers of the respective hexamers were affected by MCO. The fact that the higher order structure of Zn^{2+}-INS was not altered by MCO, as determined by CD spectroscopy and SDS-PAGE, also supports an intact hexamer after MCO. ESI-Q-TOF-MS analysis demonstrated that all oxidation products (products 1–5; Fig. 2A) resulted from the addition of either one or two oxygen atoms to INS, yielding either mono-oxidized or di-oxidized INS. As INS contains no Met, the addition of 16 a.m.u. could not be attributable to methionine sulfoxide.

Differential Susceptibility of $^{5}His_B$ and $^{10}His_B$ to MCO

The mono-oxidized B chain was sequenced by ESI-Q-TOF MS/MS to ascertain the extent of oxidation occurring at $^{5}His_B$ and $^{10}His_B$. By comparing the relative ion ratios for the mono-oxidized and native CID spectra (Fig. 4), it was evident that oxidation was specific to the two His residues. A comparison of the a_5, b_6, a_7, a_8, and b_8 fragments present in the CID spectra for the mono-oxidized B chain revealed that $^{10}His_B$ was ca. 3 times more sensitive to MCO than $^{5}His_B$ (Fig. 5 and Table II). This coincides with the fact that three $^{10}His_B$ form the metal-binding site for one Zn^{2+} molecule in the INS hexamer (17). Furthermore, Cheng and Kawakishi (19) noted a greater loss of $^{10}His_B$ than $^{5}His_B$ in the MCO of glycated-INS exposed to Cu^{2+} but did not identify products. Oxidation of $^{5}His_B$ may be related to diffusion of the oxidant from the metal binding site or transient binding of Cu^{2+} to $^{5}His_B$.

Another example demonstrating the MCO of a His residue that is not part of an intrinsic metal-binding site is provided by bGH (9). Here, ^{170}His and ^{22}His, both implicated in metal-binding by a theoretical modeling study (27), were oxidized to a greater extent than ^{20}His, which is geometrically precluded from metal-binding but is located spatially close to the metal-binding site (27). The relative ratio of His oxidation, as determined by ESI-Q-TOF MS and MS/MS, was 25:4:1 for ^{170}His:^{22}His:^{20}His (9). Importantly, some oxidation of ^{20}His occurred, possibly through diffusion of the reactive oxygen species. We note that MCO affected the metal-binding His of bGH, ^{170}His, and ^{22}His, to different extents. Different sensitivities and product patterns were also noted for the metal-binding His residues of hGH (28), ^{18}His, and ^{21}His (5). However, in contrast to ^{20}His of bGH, the equivalent ^{151}His of hGH, which is far-removed from the metal-binding site, was not affected at all.

At a Zn^{2+}/INS molar ratio comparable to the ratio in regular INS preparations, both $^{5}His_B$ and $^{10}His_B$ of INS are converted to 2-oxo-His, with $^{10}His_B$ showing a ca. 3-fold greater susceptibility to MCO than $^{5}His_B$. With only 50 μM ascorbate needed to induce significant oxidation, Zn^{2+}-INS is one of the most oxidation-sensitive proteins known so far.

ACKNOWLEDGMENTS

This research was supported by grants from the NIH (5 T32 GM 08359; PO 1 AG 12993). The Q-TOF-2 was purchased with support from KSTAR, NSF EPSCoR, and the University of Kansas.

REFERENCES

1. E. R. Stadtman. Metal ion-catalyzed oxidation of proteins: Biochemical mechanism and biologic consequences. *Free Rad. Biol. Med.* **9**:315–325 (1990).
2. E. R. Stadtman and B. S. Berlett. Reactive oxygen-mediated protein oxidation in aging and disease. *Chem. Res. Tox.* **10**:485–494 (1997).
3. K.Uchida and S. Kawakishi. Ascorbate-mediated specific oxidation of the imidazole ring in a histidine derivative. *Bioorg. Chem.* **17**:330–343 (1989).
4. K. Uchida and S. Kawakishi. 2-Oxo-histidine as a novel biologic marker for oxidatively modified proteins. *FEBS Lett.* **332**:208–210 (1993).
5. F. Zhao, E. Ghezzo-Schöneich, G. I. Aced, J. Hong, T. Milby, and C. Schöneich. Metal-catalyzed oxidation of histidine in human growth hormone. *J. Biol. Chem.* **272**:9019–9029 (1997).
6. C. Schöneich. Mechanisms of metal-catalyzed oxidation of histidine to 2-oxo-histidine in peptides and proteins. *J. Pharm. Biomed. Anal.* **21**:1093–1097 (2000).
7. S. Seibig and R. van Eldik. Kinetics of [Fe^{II}(EDTA)] oxidation by molecular oxygen revisited. New evidence for a multistep mechanism. *Inorg. Chem.* **36**:4115–4120 (1997).
8. S. A. Lewisch and R. L. Levine. Determination of 2-oxohistidine by amino acid analysis. *Anal. Biochem.* **231**:440–446 (1995).
9. S. W. Hovorka, T. D. Williams, and C. Schöneich. Characterization of the metal-binding site of bovine growth hormone through site-specific metal-catalyzed oxidation and high-performance liquid chromatography-tandem mass spectrometry. *Anal. Biochem.* **300**:206–211 (2002).
10. S. Li, T. H. Nguyen, C. Schöneich, and R. T. Borchardt. Aggregation and precipitation of human relaxin induced by metal-catalyzed oxidation. *Biochemistry* **34**:5762–5772 (1995).
11. M. Khossravi, S. J. Shire, and R. T. Borchardt. Evidence for the

involvement of histidine A(12) in the aggregation and precipitation of human relaxin induced by metal-catalyzed oxidation. *Biochemistry* **39**:5876–5885 (2000).
12. J. Jensen, K. Kuczera, S. Roy, and C. Schöneich. Metal-catalyzed oxidation of brain-derived neurotrophic factor (BDNF): Selectivity and conformational consequences of histidine modification. *Cell. Mol. Biol.* **46**:685–696 (2000).
13. S. H.Chang, G. M.Teshima, T. Milby, B. Gillece-Castro, and E. Canova-Davis. Metal-catalyzed photooxidation of histidine in human growth hormone. *Anal. Biochem.* **244**:221–227 (1997).
14. J. Brange. *Stability of Insulin. Studies on the Physical and Chemical Stability of Insulin in Pharmaceutical Formulation*, Kluwer Academic Publishers, Boston, Massachusetts 1994.
15. Y. W. Chien. Human insulin: basic sciences to therapeutic uses. *Drug Dev. Indus. Pharm.* **22**:753–789 (1996).
16. D. Brandenburg. Insulin—structure, function, design. *Exp. Clin. Endocrinol. Diabetes* **107**:S6–S12 (1999).
17. E. N. Baker, T. L. Blundell, J. F. Cutfield., S. M. Cutfield, E. J. Dodson, G. G. Dodson, D. M. Hodgkin, R. E. Hubbard, N. W. Isaacs, and C. D. Reynolds. The structure of 2Zn pig insulin crystals at 1.5 Å resolution. *Philos. Trans. R. Soc. Lond. B Biol. Sci.* **319**:369–456 (1988).
18. H. Inoue and M. Hirobe. Disulfide cleavage and insulin denaturation by active oxygen in the copper(II)/ascorbic acid system. *Chem. Pharm. Bull.* **34**:1075–1079 (1986).
19. R. Cheng and S. Kawakishi. Site-specific oxidation of histidine residues in glycated insulin mediated by Cu^{2+}. *FEBS Lett.* **223**: 759–764 (1994).
20. J. C. Evans, P. H. Morgan, M. Mahbouda, and H. J. Smith. An electron paramagnetic resonance study of native and modified freeze-dried cupric insulin hexamer. *J. Inorg. Biochem.* **11**:129–137 (1979).
21. G. D.Fasman. *Practical Handbook of Biochemistry and Molecular Biology*, CRC Press, Inc., Boca Raton, Florida 1989.
22. P. Roepstorff and J. Fohlman. Proposal for a common nomenclature for sequence ions in mass spectra of peptides. *Biomed. Mass Spectrom.* **11**:601 (1984).
23. K. Van Holde, W. C. Johnson, and P. S. Ho. *Principles of Physical Biochemistry*, Prentice-Hall, Inc., Upper Saddle River, NJ, 1998.
24. A. P. Snyder. *Interpreting Protein Mass Spectra*, Oxford University Press, New York, 2000.
25. G. R. Buettner. In the absence of catalytic metals ascorbate does not autoxidize at pH 7: Ascorbate as a test for catalytic metals. *J. Biochem. Biophys. Methods* **16**:27–40 (1988).
26. A. E.Mark, L. W. Nichol, and P. D. Jeffrey. The self-association of zinc-free bovine insulin. *Biophys. Chem.* **27**:103–117 (1987).
27. L. Carlacci, K-C. Chou, and G. M. Maggiora. A heuristic approach to predicting tertiary structure of bovine somatotropin. *Biochemistry* **30**:4389–4398 (1991).
28. B. C. Cunningham, M. G. Mulkerrin, and J. A. Wells. Dimerization of human growth hormone by zinc. *Science* **253**:545–548 (1991).